

01,05,13

The influence of the chemical composition of the ferrimagnetic layer on the features of the magnetization reversal of two-layer Tb-Dy-Co/FeNi films

© A.S. Rusalina, V.N. Lepalovskij, E.V. Kudyukov, E.A. Stepanova, G.V. Kurlyandskaya, A.V. Svalov

Institute of Natural Sciences and Mathematics,
Ural Federal University named after the First President of Russia B.N. Yeltsin,
Ekaterinburg, Russia

E-mail: anastasia.rusalina@urfu.ru, andrey.svalov@urfu.ru

Received March 6, 2025

Revised March 6, 2025

Accepted May 5, 2025

This work presents the results of the study of the magnetic properties of exchange-coupled film structures Tb-Dy-Co/FeNi obtained by magnetron sputtering. It is shown that an increase in the dysprosium content in the Tb-Dy-Co layer leads to an increase in the in-plane component of the magnetization of this layer, as well as to a decrease in the coercive force of the Tb-Dy-Co layer and a decrease in the exchange bias field of the FeNi layer at a temperature of 5 K. Changing the temperature of Tb-Dy-Co/FeNi films leads to a change in the order of magnetization reversal of the layers.

Keywords: multilayer magnetic films, interlayer exchange interaction, exchange bias, ferrimagnetism, magnetic compensation, permalloy.

DOI: 10.61011/PSS.2025.06.61701.14HH-25

1. Introduction

Multilayer film structures with exchange bias serve as the basis of spin valves [1], that in turn are the basis of many spintronic devices from magnetic recording media [2] to various magnetic field detectors [3]. The simplest spin valve consists of two ferromagnetic (FM) layers separated by a non-magnetic layer, and a fourth „pinning“ layer that, due to exchange coupling with one of the FM layers, prevents remagnetization of this „pinned“ FM layer in an external magnetic field range, consequently the hysteresis loop of the „pinned“ FM layer turns out to be shifted with respect to the zero field [2]. Antiferromagnetic materials are most often used as a „pinning“ layer material. The absence of a total magnetic moment is the advantage of such layer providing the external magnetic field resistance. It is also known that ferrimagnetic films made of amorphous rare earth — transition metal (RE-TM) alloys, i.e. Tb-Co and Dy-Co, are successfully used as an effective source of internal magnetic bias in multilayer exchange-coupled structures [4–8]. High magnetic anisotropy of Tb and Dy provides a high coercive force of these alloys. Thus, in a RE-TM/FM film system in a field range not exceeding the coercive force of the RE-TM layer, the hysteresis loop of the FM layers also turns out to be biased.

In RE-TM alloys containing heavy rare earth elements, magnetic moments of the exchange-coupled RE and TM sublattices are arranged antiparallel. With a particular composition-temperature ratio, a magnetic compensation state may occur in the film, where the spontaneous film magnetization is close to zero because the magnetic

moments of the RE and TM sublattices become equal and compensate each other. This temperature is denoted as the compensation temperature (T_{comp}) [9]. Taking into account that the exchange interaction between transition metal atoms is much higher than that for pairs of RE-TM atoms [9], it is reasonable to assume that the exchange interaction between the RE-TM and FM layers is governed by the interaction of TM atoms of these layers. Magnetic moment orientation of a particular sublattice along or against the external magnetic field direction depends on the RE-TM sample temperature because the magnetic moment of the RE sublattice prevails when $T < T_{\text{comp}}$, and the magnetic moment of the TM sublattice plays a defining role when $T > T_{\text{comp}}$. Therefore, both „negative“ and „positive“ exchange bias may be implemented in the RE-TM/FM system [6,10,11].

Despite long-lasting investigations of the magnetic properties of such RE-TM/FM systems, not all questions have been answered completely. For example, it is well known that Tb-Co and Dy-Co might have perpendicular magnetic anisotropy, particularly at temperatures near T_{comp} [5,6,12]. Thus, a situation is possible where magnetizations of the RE-TM layer and FM layer are oriented orthogonally to each other. Different models describing the exchange interaction initiation mechanism between orthogonal-magnetization layers were proposed. In one of the models, the RE-TM layer is treated as a two-phase system, and magnetizations of different phases are oriented parallel or perpendicular to the film plane, whereby the exchange bias of the FM layer is induced by the exchange interaction between the RE-TM phase with parallel magnetization orientation and the FM layer [6]. The other model implies that there is

a transition region in the RE-TM layer, within which the magnetic moment orientation of this layer changes gradually from the parallel to the perpendicular layer interface [5]. The third model may be treated as a version of the second model, which differs in that the transition interlayer region has a chiral spin structure. Occurrence of the chiral interface domain wall is treated as the consequence of the Dzyaloshinski–Moriya interaction in the RE-TM layer and the ferromagnetic exchange coupling between the RE-TM and FM layers [13].

As mentioned above, amorphous ferrimagnetic Tb-Co and Dy-Co films are successfully used as an effective source of internal magnetic bias in multilayer exchange-coupled RE-TM/FM structures [4–8]. However, such data is not available for Tb-Dy-Co films, though it is known that relation between Tb and Dy in three-component RE-TM films may modify considerably their magnetic properties, in particular, coercive force and effective atomic magnetic moment of the rare earth element [14,15]. Modification of the RE-TM layer properties by varying its composition may in turn provide new details concerning the exchange bias mechanism in the RE-TM/FM system. This paper presents the results of a study of the magnetic properties of exchange-coupled Tb-Dy-Co/FeNi film structures in a wide temperature range, including the compensation temperature of the ferrimagnetic Tb-Dy-Co layer.

2. Research methodology

Magnetron sputtering of corresponding targets was used to make Tb-Dy-Co, $Fe_{20}Ni_{80}$ films and $Tb-Dy-Co(L)/FeNi(40\text{ nm})$ bilayers, where the layer thickness L was 20 nm or 40 nm. Corning cover slips were used as substrates. Tb-Dy-Co layers were deposited by co-sputtering of Tb, Dy and Co single-component targets. Modification of electric power supplied to the targets made it possible to vary the chemical composition of these layers, the amount of Co in the $(Tb_xDy_{100-x})_{20}Co_{80}$ layers was fixed and equal to 80 at.%, and the relation between two rare-earth components, Tb and Dy, varied, their percentage varied from 0 to 100 at.%. To prevent oxidation, all samples were protected by buffer and top Ta layers (5 nm). During film deposition, 250 Oe permanent magnetic field was applied in the substrate plane to generate an induced uniaxial magnetic anisotropy in the layers. Elemental composition of films was controlled using the Nanohunter X-ray fluorescence spectrometer with error of 0.5 at.%. Hysteresis loops and temperature dependences of film magnetization in the temperature range from 5 to 300 K were measured on the MPMS-7XL measuring system.

3. Findings

Hysteresis loops measured in different directions in the plane of both Tb-Dy-Co and FeNi single-layer and

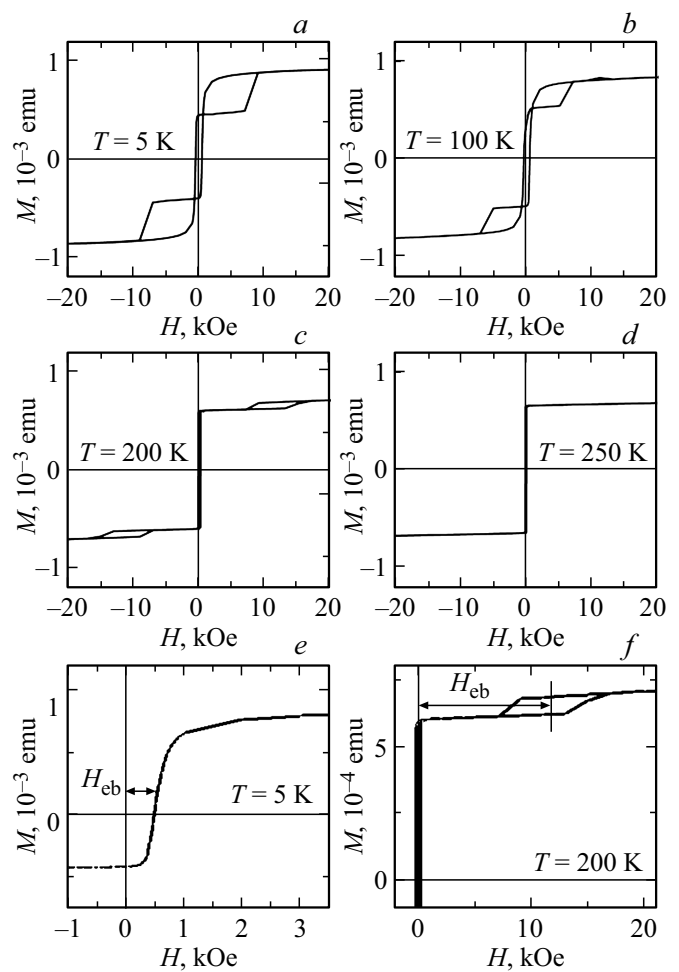


Figure 1. Hysteresis loops measured along EA in the $(Tb_{32}Dy_{68})_{20}Co_{80}/FeNi(40\text{ nm})$ film at different temperatures (a–d). A partial hysteresis loop corresponding to remagnetization of the FeNi layer at $T = 5\text{ K}$ (e). A scaled up part of the hysteresis loop measured at $T = 200\text{ K}$ (f).

Tb-Dy-Co/FeNi two-layer film samples showed that induced magnetic anisotropy was formed in the films. The anisotropy easy axis (EA) coincides with the orientation of the process magnetic field that existed during film sputtering.

Figure 1 shows hysteresis loops measured along EA in the $(Tb_{32}Dy_{68})_{20}Co_{80}/FeNi(40\text{ nm})$ film at different temperatures.

The figure also shows a partial hysteresis loop corresponding to remagnetization of the FeNi layer at $T = 5\text{ K}$ (Figure 1, e) and a scaled up part of the hysteresis loop measured at $T = 200\text{ K}$ (Figure 1, f) where methods to determine the exchange bias field H_{eb} are marked. For a hysteresis loop corresponding to the FeNi layer remagnetization, this is the field coordinate of a point at half amplitude of the loop; and in the second case this is the field coordinate of the center of the partial hysteresis loop. Such loops were also observed for Tb-Dy-Co/FeNi films with other Tb-Dy ratio. At $T < 250\text{ K}$, the step-like shape

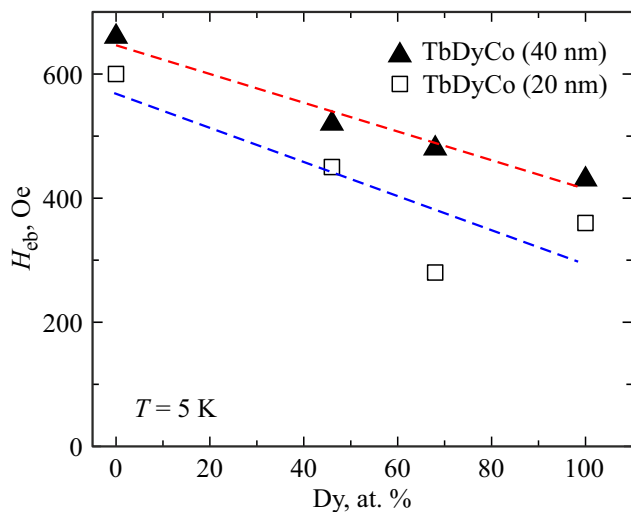


Figure 2. Dependence of the exchange bias field on composition (Tb-Dy ratio) and $(Tb_xDy_{100-x})_{20}Co_{80}$ layer thickness of the Tb-Dy-Co/FeNi (40 and 20 nm) two-layer film at $T = 5$ K.

of loops results from layer-by-layer remagnetization of the sample. Magnetization of the FeNi layer varies a little in the given interval, therefore, a hysteresis loop measurement signal corresponding to the layer remagnetization also varies a little. Magnetization of the Tb-Dy-Co layer at $T = 5$ K is approximately 3 times as low as that of the FeNi layer and decreases monotonously as the temperature increases up to T_{comp} . Thus, compliance of different loop segments with the remagnetization of a particular layer can be easily established taking into account the magnetization an layer thickness.

At $T = 5$ K, the total magnetic moment of the Tb-Dy-Co layer is defined by the rare-earth component moment. Thus, in the absence of external magnetic field, magnetic moments of the Tb-Dy-Co and FeNi layers are antiparallel. Strong external field arranges magnetic moments of layers parallel to each other. In addition, as it was illustrated by so-called „spin springs“ [16,17], a domain boundary type magnetic inhomogeneity is formed in the interlayer region. Its energy may be estimated using the known expression $\sigma_w = 4(AK_u)^{1/2}$, where A is the exchange interaction constant, K_u is the anisotropy constant [18]. Substitution of A and K_u taken from the literature and corresponding to the Tb-Dy-Co and FeNi layers into this expression showed that σ_w will be higher by an order of magnitude, if inhomogeneity is formed in the FeNi layer (for example, 0.2 erg/cm 2 and 2.5 erg/cm 2 , respectively). This result suggests that the boundary is formed in the FeNi layer.

Let's compare the remagnetization process of the sample with hysteresis loop segments starting from the maximum positive field. As the external field decreases, magnetic moments within the FeNi layer are rotated, the interlayer magnetic interface disappears and the magnetic moments of the Tb-Dy-Co and FeNi layers again turn out to be

arranged antiparallel. External field reversal and increase stabilize the magnetic moment orientation of the FeNi layer, but a particular field strength leads to remagnetization of the Tb-Dy-Co layer.

Analysis of the hysteresis loops measured at $T = 5$ K for samples with different compositions of the Tb-Dy-Co layer made it possible to plot the dependence of the exchange bias field H_{eb} on composition (Tb-Dy ratio) (Figure 2).

It is shown that an increase in the Dy concentration leads to a considerable decrease of H_{eb} . Possible causes of this dependence may include composition dependence of both M of the Tb-Dy-Co layer and magnetization vector orientation with respect to the sample plane. On the one hand, the magnetic moment of Dy atom is higher than that of Tb. On the other hand, sperimagnetic structure is inherent in the Tb-Dy-Co type amorphous films and the effective magnetization depends on the angular opening of sperimagnetism cone that can also depend on the Tb-Dy ratio [19–21]. Magnetization vector orientation with respect to the sample plane is in turn defined by the competition between the perpendicular magnetic anisotropy and form anisotropy depending on M . Figure 3 shows the hysteresis loops for the $Tb_{20}Co_{80}$, $(Tb_{32}Dy_{68})_{20}Co_{80}$ and $Dy_{20}Co_{80}$ films measured when the external magnetic field is oriented in the sample plane along EA and perpendicular to the sample plane at $T = 5$ K.

For the Tb-Co film, a loop measured with the external magnetic field oriented perpendicular to the sample plane has a shape typical of a so-called „supercritical state“, which a system of domains corresponds to in the absence of an external field. Magnetic moments in this system deviate from normal at the angle φ smaller than 90° , their planar components are the same and normal components are alternating [18,22,23]. φ may be estimated using $\cos \varphi = M_r/M_s$, where M_r is the residual magnetization, M_s is the saturation magnetization. In this case $M_r = 0.8M_s$, which corresponds to $\varphi \approx 37^\circ$. For the $(Tb_{32}Dy_{68})_{20}Co_{80}$ film, the shapes of the loops measured in two directions and the values of M_r are very close to each other (Figure 3, b), and for the $Dy_{20}Co_{80}$ film, the loops indicate that the magnetization is oriented in the sample plane (Figure 3, c). Thus, an increase in the Dy concentration leads to an increase in the planar magnetization components without an external field at $T = 5$ K. This result in turn suggests that the planar component in the Tb-Dy-Co layer is not a governing factor of H_{eb} (Figure 2). Such factor is possibly the coercive force H_c of the Tb-Dy-Co layer assuming that the interlayer magnetic inhomogeneity is localized not exclusively in the FeNi layer, but also partially in the Tb-Dy-Co layer, in this case H_{eb} will also depend on the magnetic hardness of the Tb-Dy-Co layer. Figure 4 shows the dependence of H_c on the composition, it can be seen that the variation of H_c has the same trend as H_{eb} as the Dy concentration increases (Figure 2).

Temperature dependences M_r and H_c of the Tb-Dy-Co layers have their minimum and maximum, respectively,

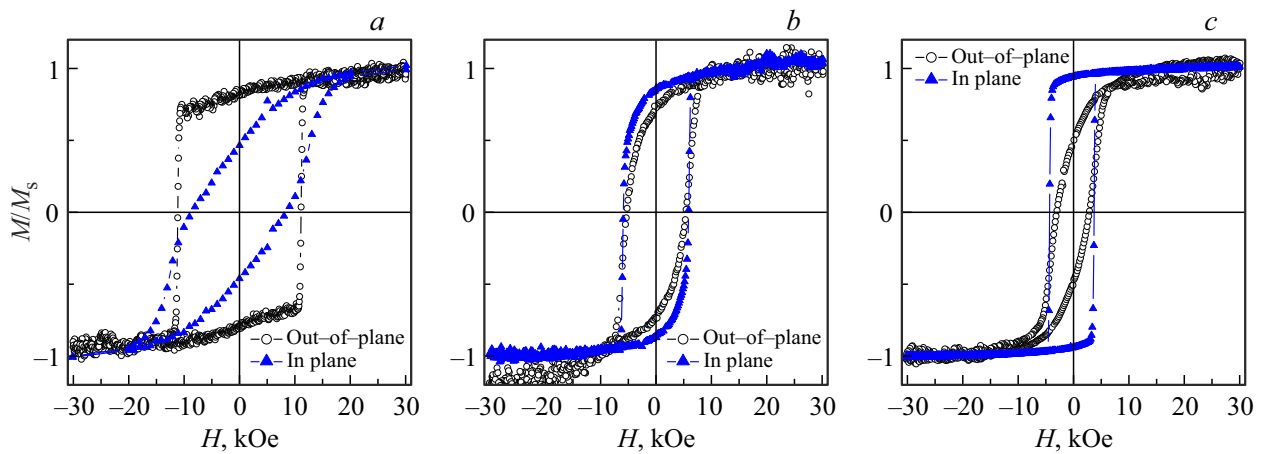


Figure 3. Hysteresis loops measured when the external magnetic field is oriented along and perpendicular to the sample plane for $\text{Tb}_{20}\text{Co}_{80}$ (a), $(\text{Tb}_{32}\text{Dy}_{68})_{20}\text{Co}_{80}$ (b) and $\text{Dy}_{20}\text{Co}_{80}$ (c) films at $T = 5$ K. Film thickness is 20 nm.

near T_{comp} , which is typical of ferrimagnetic materials. As an example, Figure 5 shows $M_r(T)$ and $H_c(T)$ for the $\text{Dy}_{20}\text{Co}_{80}$ film. Similar dependences were observed for the Tb-Dy-Co films with all compositions addressed in the work.

As follows from the data in Figure 1, an increase in the temperature of the Tb-Dy-Co/FeNi two-layer sample leads to a change of the hysteresis loop shape, which reflects the change of the film remagnetization scenario. Within the given temperature range, the magnetization of the FeNi layer varies a little as opposed to the Tb-Dy-Co layer (Figure 5). This modifies the Zeeman energy balance, magnetic anisotropy of layers and interlayer exchange resulting in the change of the layer remagnetization sequence. If, at $T < 200$ K, the magnetization orientation of the FeNi layer changed first as the field decreased after magnetization of the sample by the maximum field, then, at $T \geq 200$ K, the Tb-Dy-Co layer is remagnetized first (Figure 1).

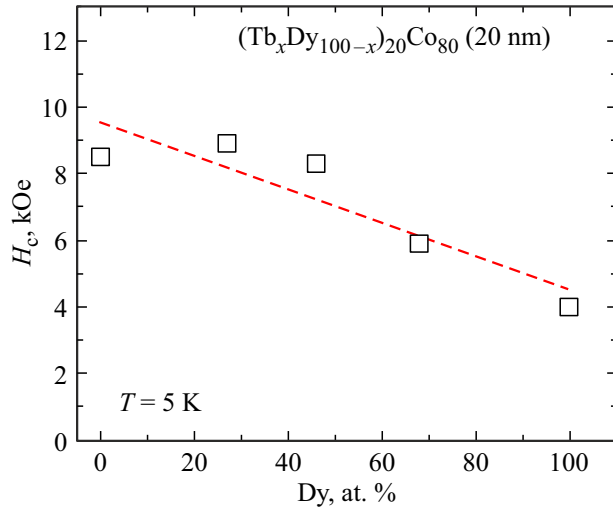


Figure 4. Dependence of the coercive force on composition (Tb-Dy ratio) of the $(\text{Tb}_x\text{Dy}_{100-x})_{20}\text{Co}_{80}$ (20 nm) films at $T = 5$ K.

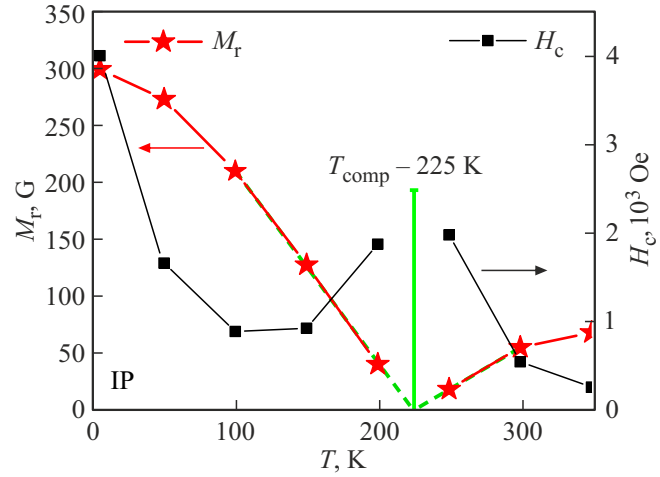


Figure 5. Temperature dependences of magnetization and coercive force for the $\text{Dy}_{20}\text{Co}_{80}$ film.

Thus, the temperature range below the compensation temperature may be divided into two layer remagnetization sequence regions (Figure 6, a). Let's consider the causes of change of the remagnetization sequence in greater detail using a two-layer system with a magnetically hard $\text{Dy}_{20}\text{Co}_{80}$ layer as an example. In both regions with a positive field higher than 15 kOe, the system attains the saturation, where the magnetic moments of both layers are codirectional. Unlike the classical spin spring case [16], remagnetization of the first of the layers always takes place even at the field direction, in which the system was magnetized before the saturation. In region I, remagnetization starts from the magnetically soft FeNi layer. At $T = 5$ K, magnetization of the FeNi (~ 800 G) layer is approximately three times as high (Figure 6, a), and the thickness is two times as high than those of the Dy-Co layer, therefore, the Zeeman energy of the FeNi layers is much higher. But the coercive force of the Dy-Co layer is three orders of magnitude as high

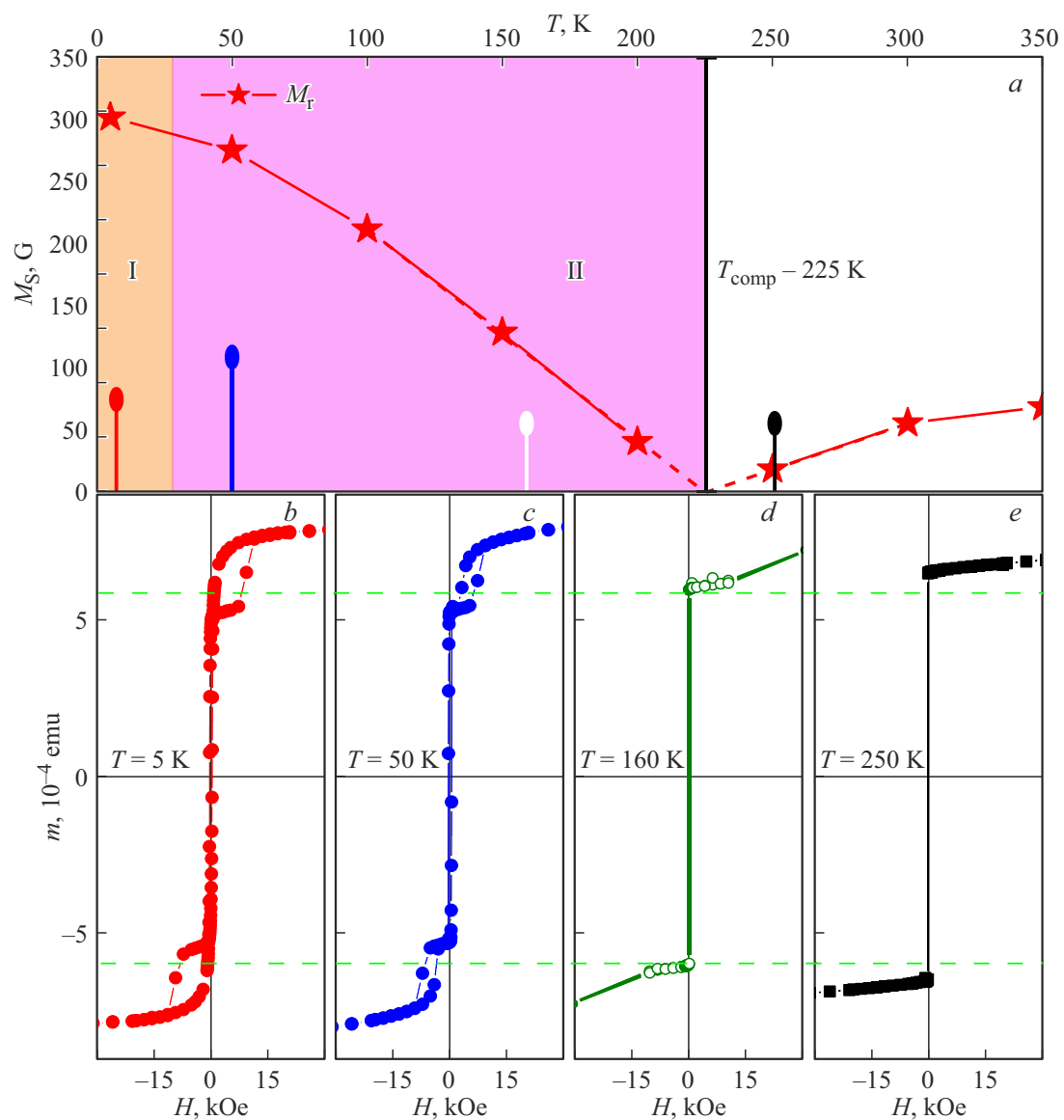


Figure 6. Temperature dependence of the saturation magnetization — *a*; hysteresis loops for the Dy₂₀Co₈₀(20 nm)/Fe₂₀Ni₈₀(40 nm) film at different temperatures — *b, c, d, e*, the field is applied in the film plane.

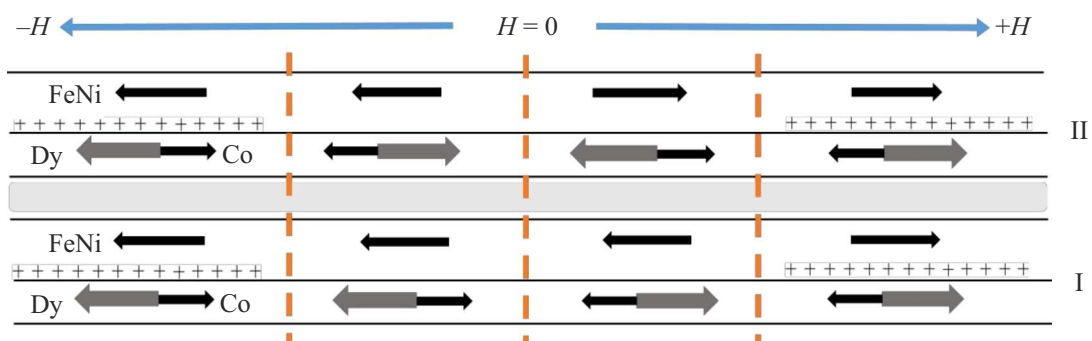


Figure 7. Scheme of magnetic moment remagnetization of the structure layers in the first and second temperature regions.

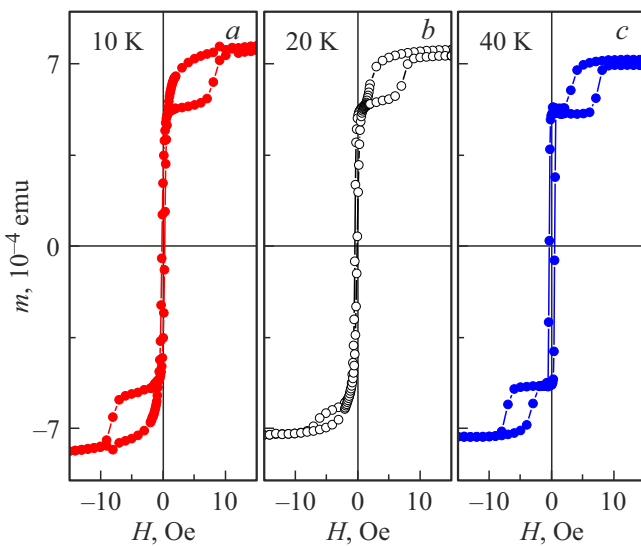


Figure 8. Hysteresis loops for the $\text{Dy}_{20}\text{Co}_{80}$ (20 nm)/ $\text{Fe}_{20}\text{Ni}_{80}$ (40 nm) film demonstrating the system remagnetization sequence change as the sample temperature varies. In the text, the hysteresis loops are analyzed for motion from positive to negative fields.

as that of FeNi (Figure 5). Eventually, in this case it is more energetically favorable for the Dy-Co/FeNi two-layer structure if the energy gain resulting from the disappearance of the interlayer magnetic inhomogeneity is induced by the FeNi layer remagnetization.

Subsequent sign reversal and increase in the external field facilitate stabilization of the FeNi layer magnetization orientation and Dy-Co layer remagnetization at $|H| > 10$ kOe (Figure 6, b). In the second temperature region ($T > 10$ K), the situation is reversed — the magnetically hard Dy-Co layer is the first to respond to the field strength change. This is because both the magnetic moment and coercive force

of the Dy-Co layer decrease as the temperature increases (Figure 6, a). This modifies the Zeeman energy balance, magnetic anisotropy of layers and interlayer exchange, consequently, the Dy-Co layer remagnetization becomes energetically favorable, while the magnesium orientation of the FeNi layer remains stabilized by the external magnetic field. When the field direction changes, the Dy-Co/FeNi system is remagnetized as a whole in relatively weak field, and as the field further increases, the Dy-Co layer is remagnetized with newly formed magnetic inhomogeneity near the layer interface (Figure 6, c, d). Scheme of remagnetization in different temperature regions is shown in Figure 7.

A temperature region, where the remagnetization sequence is changed, is of particular interest. Figure 8 shows the hysteresis loops measured successively during system cooling at 10 K intervals. Sample remagnetization processes corresponding to the loops measured at 10 K and 40 K (Figure 8, a, c) are described above.

The layer remagnetization sequence probably changes within some temperature interval, rather than suddenly at a particular temperature. Thus, when analyzing the hysteresis loop measured at $T = 20$ K, it is difficult to say with certainty which of the layers starts to be remagnetized first as the field decreases from the maximum negative value (third quadrant). This may be caused by some inhomogeneity in the sample area of the interlayer interface composition induced by interdiffusion between layers. Some loop asymmetry (difference in the shape of partial hysteresis loops in the first and third quadrants) may also result from magnetic history of the sample during measurements. In particular, before measuring the hysteresis loop at $T = 20$ K, the sample was magnetized to saturation at $T = 40$ K and cooled to 20 K in this state. Probably in this case a magnetic configuration of the interlayer interface, that facilitates some behavior asymmetry of the sample in the unlike magnetic field, was „frozen“.

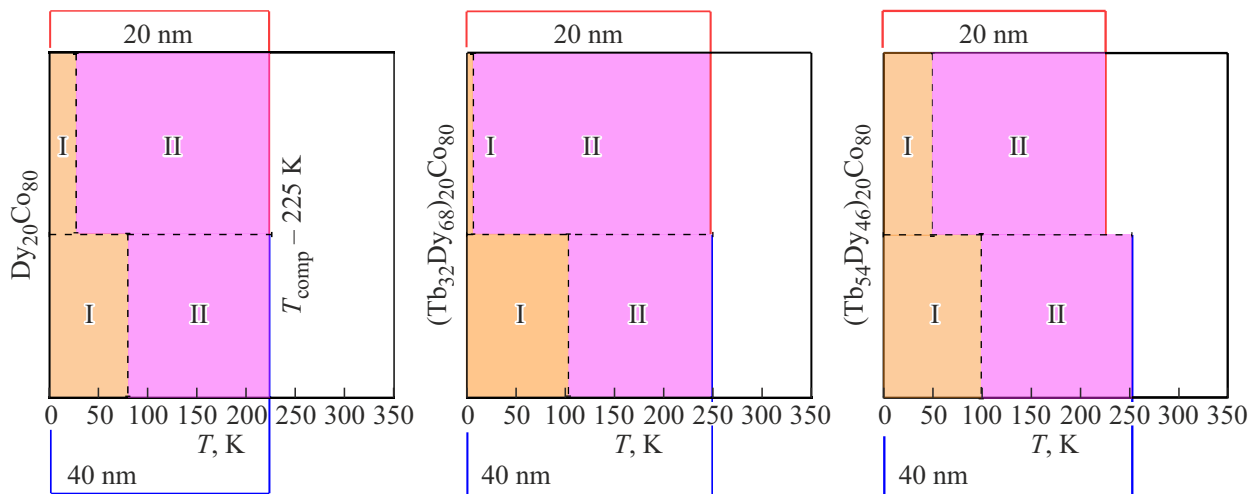


Figure 9. Temperature ranges of different layer remagnetization sequence regions in the Tb-Dy-Co/FeNi films with different compositions of the Tb-Dy-Co film layer. Upper diagrams are for the Tb-Dy-Co layer thickness of 20 nm, lower ones are for 40 nm.

At $T > T_{\text{comp}}$, the total magnetic moment of the Tb-Dy-Co layer is defined by the Co sublattice's magnetic moment. Thus, in the absence of the external magnetic field, magnetizations of the Tb-Dy-Co and FeNi layers are ferromagnetically ordered and act as a unit when the field changes (Figure 1, *d* and 6, *e*).

Change in the composition and thickness of the magnetically hard Tb-Dy-Co layer doesn't modify the Tb-Dy-Co/FeNi film remagnetization scenario, but shifts the boundaries of the temperature regions, where the layer remagnetization sequence is modified (Figure 9).

4. Conclusion

The study has demonstrated that the planar component of magnetization in the Tb-Dy-Co layer of exchange-coupled Tb-Dy-Co/FeNi two-layer films was not a factor defining the magnitude of the exchange bias field H_{eb} . Coercive force of the Tb-Dy-Co layer most likely acts as such factor. The layer remagnetization sequence depends on the sample temperature and is defined by the Zeeman energy balance, magnetic anisotropy of layers and interlayer exchange.

Funding

The results were obtained as part of state assignment FEUZ-2023-0020 of the Ministry of Science and Higher Education of the Russian Federation.

Conflict of interest

The authors declare that they have no conflict of interest.

References

- [1] L.I. Naumova, M.A. Milyaev, T.A. Chernyshova, V.V. Proglyado, I.Yu. Kamensky, V.V. Ustinov. *FTT* **56**, 1082 (2014). (in Russian).
- [2] B. Dieny, in: M. Johnson (Ed.), *Spin Valves in Magnetoelectronics*, Elsevier, Amsterdam (2004) 67–149.
- [3] P.P. Freitas, R. Ferreira, S. Cardoso. *Proc. IEEE* **104**, 1894 (2016).
- [4] V.A. Seredkin, G.I. Frolov, V.Yu. Yakovchuk. *Pis'ma ZhTF*, **1446**, 1983 (2005). (in Russian).
- [5] W.C. Cain, M.H. Kryder. *J. Appl. Phys.* **67**, 5722 (1990).
- [6] G.I. Frolov, V.Yu. Yakovchuk, V.A. Seredkin, R.S. Iskhakov, S.V. Stolyar, V.V. Polyakov. *ZhTF*, **75** (69), 2005 (2005). (in Russian)
- [7] V.O. Vaskovsky, A.V. Svalov, K.G. Balymov, N.A. Kulesh. *FMM* **113**, 908 (2012). (in Russian).
- [8] C. Vogler, M. Heigl, A.-O. Mandru, B. Hebler, M. Marioni, H.J. Hug, M. Albrecht, D. Suess. *Phys. Rev. B* **102**, 014429 (2020).
- [9] R. Hasegawa, R.J. Gambino, R. Ruf. *Appl. Phys. Lett.* **27**, 512 (1975).
- [10] T. Hauet, S. Mangin, F. Montaigne, J.A. Borchers, Y. Henry. *Appl. Phys. Lett.* **91**, 022505 (2007).
- [11] A.V. Svalov, V.N. Lepalovsky, E.A. Stepanova, I.A. Makarochkin, V.O. Vaskovsky, A. Larañaga, G.V. Kurlyandskaya. *FTT* **63**, 1198 (2021). (in Russian).
- [12] V.O. Vaskovsky, K.G. Balymov, A.V. Svalov, N.A. Kulesh, E.A. Stepanova, A.N. Sorokin. *FTT* **53**, 2161 (2011). (in Russian).
- [13] K. Chen, A. Philippi-Kobs, V. Lauter, A. Vorobiev, E. Dyadkina, V.Yu. Yakovchuk, S. Stolyar, D. Lott. *Phys. Rev. A* **12**, 024047 (2019).
- [14] P.I. Williams, D.G. Lord, P.J. Grundy. *J. Appl. Phys.* **75**, 5257 (1994).
- [15] K.G. Balymov, E.V. Kudyukov, V.O. Vas'kovskiy, O.A. Adanakova, N.A. Kulesh, E.A. Stepanova, A.S. Rusalina. *J. Phys. Conf.* **1389**, 012014 (2019).
- [16] E.E. Fullerton, J.S. Jiang, S.D. Bader. *J. Magn. Magn. Mater.* **200**, 392 (1999).
- [17] D. Chumakov, R. Schäfer, D. Elefant, D. Eckert, L. Schultz, S.S. Yan, J.A. Barnard. *Phys. Rev. B* **66**, 134409 (2002).
- [18] A. Hubert, R. Schäfer. *Magnetic domains. The Analysis of Magnetic Microstructures*. Springer, Berlin (1998). 696 p.
- [19] J. Yu, L. Liu, J. Deng, C. Zhou, H. Liu, F. Poh, J. Chen. *J. Magn. Magn. Mater.* **487**, 1653161 (2019).
- [20] A.V. Svalov, I.A. Makarochkin, E.V. Kudyukov, E.A. Stepanova, V.O. Vaskovsky, A. Larañaga, G.V. Kurlyandskaya. *FMM* **125**, 83 (2021). (in Russian).
- [21] V.O. Vaskovsky, E.V. Kudyukov, E.A. Stepanova, E.A. Kravtsov, O.A. Adanakova, A.S. Rusalina, K.G. Balymov, A.V. Svalov. *FMM* **513**, 83 (2021). (in Russian).
- [22] L.M. Álvarez-Prado, J.M. Alameda. *Physica B* **343**, 241 (2004).
- [23] V.O. Vaskovsky, A.N. Gorkovenko, O.A. Adanakova, A.V. Svalov, N.A. Kulesh, E.A. Stepanova, E.V. Kudyukov, V.N. Lepalovsky. *FMM* **120**, 1151 (2019). (in Russian).

Translated by E.Illinskaya